Chun-Hua Zhang; Jun-Wei Jin; Hai-Wei Sun; Qin Sheng

A spatially sixth-order hybrid $L1$-CCD method for solving time fractional Schrödinger equations

Applications of Mathematics, Vol. 66 (2021), No. 2, 213–232

Persistent URL: http://dml.cz/dmlcz/148721

A SPATIALLY SIXTH-ORDER HYBRID $L1$-CCD METHOD FOR SOLVING TIME FRACTIONAL SCHRÖDINGER EQUATIONS

Chun-Hua Zhang, Macau, Jun-Wei Jin, Zhengzhou,
Hai-Wei Sun, Macau, Qin Sheng, Waco

Received December 4, 2019. Published online December 16, 2020.

Abstract. We consider highly accurate schemes for nonlinear time fractional Schrödinger equations (NTFSEs). While an $L1$ strategy is employed for approximating the Caputo fractional derivative in the temporal direction, compact CCD finite difference approaches are incorporated in the space. A highly effective hybrid $L1$-CCD method is implemented successfully. The accuracy of this linearized scheme is order six in space, and order $2-\gamma$ in time, where $0<\gamma<1$ is the order of the Caputo fractional derivative involved. It is proved rigorously that the hybrid numerical method accomplished is unconditionally stable in the Fourier sense. Numerical experiments are carried out with typical testing problems to validate the effectiveness of the new algorithms.

Keywords: nonlinear time fractional Schrödinger equations; $L1$ formula; hybrid compact difference method; linearization; unconditional stability

MSC 2020: 65M06, 65M20, 65M60

1. Introduction

In past decades, fractional differential equations have widely attracted the attention of researchers from different fields due to their outstanding memory and hereditary properties in multi-physical modeling and approximations. They may offer more precise descriptions in the sciences than traditional differential equations [1], [18], [40], [42]. Consequently, fractional differential equations have become popular in engineering, physical, biological, geological, and financial system applications, see [2],

The first three authors are supported in part by the Science and Technology Development Fund and University of Macau, Macau, through Research Grants (No. 0118/2018/A3) and (MYRG2018-00015-FST). The last author is supported in part by a Research Award from the CAS, Baylor University, USA.

DOI: 10.21136/AM.2020.0339-19

[12], [24], [34]. Results in fractional derivative analysis and computations, including the construction of analytical solutions of fractional partial differential equations, can be found in numerous recent publications. Since closed-form analytical solutions are available for fractional differential equations only in extremely limited cases, it has become imminent that highly accurate and reliable numerical methods must be developed.

Among the many fractional equations, Schrödinger equations stand out for their fundamental roles in quantum mechanics [11]. Naber initially noticed that the first order temporal derivative can be generalized via a γth-order Caputo fractional derivative in a Schrödinger equation for better modeling approximations [32]. Naber further proved that such a fractional order Schrödinger equation is a time-dependent Hamiltonian. Solution approximations are necessary for a better understanding of fractional order Schrödinger equations. To this end, asymptotic approximations of NTFSE solutions were constructed with zero and nonzero trapping potentials [23]. The Adomian decomposition method as an alternative approach for obtaining analytic and approximate solutions was proposed later [33]. Wei et al. presented and analyzed an implicit fully discrete local discontinuous Galerkin finite element method for solving NTFSEs [40]. A novel Jacobi spectral collocation method in combination with the operational matrix of fractional derivatives was investigated [3]. Standard and shifted Grünwald formulas were considered [42]. Further, Shivanian and Jafarabadia invented a spectral meshless radial point interpolation technique for NTFSEs [35]. A linearized $L1$-Galerkin finite element strategy for attacking multidimensional NTFSEs was recommended by Li et al. recently [28]. Although spatially fourth-order methods were investigated in multiple publications [6], [7], [10], [16], [37], [39] for a number of time-fractional partial differential equations, the study of higher order numerical procedures for NTFSEs has been in its infancy.

On the other hand, Chu and Fan introduced a combined compact difference (CCD) method in 1998, see [9]. In such an approach, the first- and second-order derivatives of the solution functions are assumed to be two different variables. Combining with the solution function, a triple-tridiagonal system may be accomplished for the original partial differential equation. Moreover, a CCD strategy requires only three spatial mesh points to achieve a sixth-order accuracy, which is favorable for solving fractional differential equations. As an application, Gao and Sun constructed a three-point CCD scheme based on a global Hermitian polynomial with continuous first and second-order derivatives for time-fractional advection-diffusion equations [13], [14]. The algorithm attains a sixth-order accuracy in space successfully. Moreover, a spatially sixth-order alternating direction implicit (ADI) method for two-dimensional cubic Schrödinger equations was given by Li et al. [27]. Based on it, He and Pan acquired a three-level linearly implicit ADI-CCD scheme for solving a generalized

Schrödinger equation with variable coefficients [21]. For more detailed information about the CCD strategies, a reader is referred to [8], [9], [19], [20], [26], [36], [38].

To the best of our knowledge, however, CCD approximations have never been successfully incorporated with powerful $L1$ formula for solving NTFSEs. This motivates our investigation. A highly effective hybrid and linearized structure is proposed. The resulted numerical method achieves a sixth-order accuracy in space, taking advantages of the CCD, and $(2-\gamma)$th order accuracy in time due to $L1$ configurations. The unconditional stability of this novel method is proved via a Fourier analysis. Numerical experiments will be given to illustrate and demonstrate the anticipated accuracy and effectiveness.

The remainder of this paper is organized as follows: In Section 2, the linearized and spatially sixth-order CCD strategy is introduced and discussed. Our stability analysis is given in Section 3. Computational experiments are presented in Section 4. Finally, brief remarks and conclusions are given in Section 5.

2. $L1$ formulation and linear CCD method

We consider the following NTFSE (see [30], [40]):

$$\mathrm{i}\frac{\partial^\gamma \Psi}{\partial t^\gamma} + \alpha\frac{\partial^2 \Psi}{\partial x^2} + P|\Psi|^2\Psi + V(x)\Psi = f(x,t), \quad (x,t) \in \Omega \times (0,T], \tag{2.1}$$

together with the initial condition

$$\Psi(x,0) = \Psi_0(x), \quad x \in \Omega, \tag{2.2}$$

and a periodic boundary condition

$$\Psi(x+L,t) = \Psi(x,t), \quad (x,t) \in \Omega \times [0,T], \tag{2.3}$$

where i is the imaginary unit, α, P are real constants, Ω is a closed interval, L is the period, $V(x)$ is the real-valued trapping potential function. Both $f(x,t)$ and $\Psi_0(x)$ are assumed to be given sufficiently smooth complex functions, and $\Psi(x,t)$ be the unknown complex solution. The temporal fractional derivative $\partial^\gamma \Psi/\partial t^\gamma$ is defined in the Caputo sense [31]:

$$\frac{\partial^\gamma \Psi(x,t)}{\partial t^\gamma} = \begin{cases} \dfrac{1}{\Gamma(1-\gamma)} \displaystyle\int_0^t \frac{\partial \Psi(x,s)}{\partial s}(t-s)^{-\gamma}\,\mathrm{d}s & \text{if } 0 < \gamma < 1, \\ \dfrac{\partial \Psi(x,t)}{\partial t} & \text{if } \gamma = 1, \end{cases} \tag{2.4}$$

where $\Gamma(\cdot)$ is the Gamma function.

2.1. $L1$ **formula.** For the sake of simplicity, we may rewrite (2.1) as the following

$$\frac{\partial^\gamma \Psi}{\partial t^\gamma} - \mathrm{i}\alpha \frac{\partial^2 \Psi}{\partial x^2} - \mathrm{i}P|\Psi|^2\Psi - \mathrm{i}V(x)\Psi = -\mathrm{i}f(x,t). \tag{2.5}$$

In order to get the numerical solution of this periodic initial-boundary value problem, we may restrict it to a bounded domain $[0, L] \times [0, T]$. We consider a temporal discretization. Herewith we divide $[0, T]$ to N subintervals, with the temporal step $\tau = T/N$. Denote $t_n = n\tau$, $n = 0, 1, \ldots, N$. Let Ψ^n be an approximation of $\Psi(t_n)$.

Further, for the fractional derivative in (2.5), we need the following [16]:

$$\mathcal{D}_t^\gamma \Psi(t_n) = \frac{\tau^{-\gamma}}{\Gamma(2-\gamma)} \Big[\lambda_0 \Psi(t_n) - \sum_{m=1}^{n-1} (\lambda_{n-m-1} - \lambda_{n-m}) \Psi(t_m) - \lambda_{n-1} \Psi(t_0) \Big], \tag{2.6}$$

where $\lambda_l = (l+1)^{1-\gamma} - l^{1-\gamma}$, $l \geqslant 0$. The above is frequently referred to as the $L1$ formula. It ensures an order of accuracy $(2-\gamma)$ (see [27]).

We also need the following lemma.

Lemma 2.1 ([16], [37]). *Suppose that* $\Psi(t) \in C^2[0, t_n]$ *and* $0 < \gamma < 1$. *If*

$$\overline{R}(\Psi(t_n)) := \frac{1}{\Gamma(1-\gamma)} \int_0^{t_n} \frac{\Psi'(s)}{(t_n - s)^\gamma} \, \mathrm{d}s - \mathcal{D}_t^\gamma \Psi(t_n),$$

then

$$|\overline{R}(\Psi(t_n))| \leqslant \frac{1}{\Gamma(2-\gamma)} \Big[\frac{1-\gamma}{12} + \frac{2^{2-\gamma}}{2-\gamma} - (1 + 2^{-\gamma}) \Big] \max_{0 \leqslant t \leqslant t_n} |\Psi''(t)| \tau^{2-\gamma}.$$

Utilizing (2.6) and the lemma, we acquire the following temporal discretization of (2.5) at $t = t_n$:

$$\mathcal{D}_t^\gamma \Psi^n - \mathrm{i}\alpha \Big(\frac{\partial^2 \Psi}{\partial x^2} \Big)^n - \mathrm{i}P|\Psi^n|^2\Psi^n - \mathrm{i}V\Psi^n = -\mathrm{i}f^n + \mathcal{O}(\tau^{2-\gamma}). \tag{2.7}$$

2.2. Linearized CCD method. Consider the spatial discretization of (2.7). A linearization strategy is used for the nonlinear term. To this end, we uniformly divide $[0, L]$ to M subintervals, where $M > 0$ is an integer. Denote $x_j = jh$, $j = 0, 1, \ldots, M$, where $h = L/M$. We further denote Ψ_j^n, $(\Psi_x)_j^n$ and $(\Psi_{xx})_j^n$ for Ψ, $\partial\Psi/\partial x$ and $\partial^2\Psi/\partial x^2$ at grid point (x_j, t_n), respectively. Drop the truncated error in (2.7). We have

$$\mathcal{D}_t^\gamma \Psi_j^n - \mathrm{i}\alpha(\Psi_{xx})_j^n - \mathrm{i}P|\Psi_j^n|^2\Psi_j^n - \mathrm{i}V_j\Psi_j^n = -\mathrm{i}f_j^n. \tag{2.8}$$

Now we consider the CCD approximation in the space. To this end, similar to [36], we proceed ahead with

$$\frac{7}{16}[(\Psi_x)_{j+1}+(\Psi_x)_{j-1}]+(\Psi_x)_j-\frac{h}{16}[(\Psi_{xx})_{j+1}-(\Psi_{xx})_{j-1}] = \frac{15}{16h}(\Psi_{j+1}-\Psi_{j-1})+\mathcal{O}(h^6), \tag{2.9}$$

$$\frac{9}{8h}[(\Psi_x)_{j+1}-(\Psi_x)_{j-1}]-\frac{1}{8}[(\Psi_{xx})_{j+1}+(\Psi_{xx})_{j-1}]+(\Psi_{xx})_j = \frac{3}{h^2}(\Psi_{j+1}-2\Psi_j+\Psi_{j-1})+\mathcal{O}(h^6) \tag{2.10}$$

for $j=1,2,\ldots,M$ under periodic boundary constraints

$$\Psi_0=\Psi_M,\quad \Psi_1=\Psi_{M+1},\quad (\Psi_x)_0=(\Psi_x)_M,\quad (\Psi_x)_1=(\Psi_x)_{M+1},$$
$$(\Psi_{xx})_0=(\Psi_{xx})_M,\quad (\Psi_{xx})_1=(\Psi_{xx})_{M+1}.$$

Therefore, the CCD system, consisting of (2.7), and (2.9), (2.10) possesses $3M$ equations with $3M$ unknowns to solve.

However, we still face another difficulty in solving the NTFSE. It is noticed that if the real constant $P\neq 0$, then (2.8) is nonlinear.

In fact, this challenge has attracted a tremendous amount of recent attentions from the community [4], [5], [27], [29]. There are two popular tools to use in the situation: an iterative method or a linearization. Bear in mind that our non-local time-fractional operator requires historical memories. An iterative method may imply the need for large storage and CPU/GPU time, especially when the number of time advancements is relatively large. Thus, a linearization should be more economical for handling the fractional nonlinearity. Among existing linearization procedures, we prefer a suitable extrapolation procedure [4], [41]. For this purpose, we hybridize our CCD approach together with a selected extrapolation for solving NTFSEs including (2.1). Denote

$$|\Psi^n|\approx|2\Psi^{n-1}-\Psi^{n-2}|:=|\Psi^e|. \tag{2.11}$$

Then, a linearization of (2.8) leads to

$$\mathcal{D}_t^\gamma\Psi_j^n-\mathrm{i}\alpha(\Psi_{xx})_j^n-\mathrm{i}P|\Psi_j^e|^2\Psi_j^n-\mathrm{i}V_j\Psi_j^n=-\mathrm{i}f_j^n. \tag{2.12}$$

Since the extrapolation is of second-order accuracy in time, i.e., $|\Psi^n|=|\Psi^e|+\mathcal{O}(\tau^2)$, the temporal accuracy of (2.12) must be $\mathcal{O}(\tau^{2-\gamma})$. Further, (2.9)–(2.10) and (2.12) introduce a three-level, or leapfrog, method. Therefore both Ψ^0 and Ψ^1 must be

available before our computations. The value Ψ^1 is usually generated via a straightforward iteration [27].

Denote

$$\mu = \tau^\gamma \Gamma(2-\gamma). \tag{2.13}$$

An application of the hybrid $L1$-CCD procedure (2.9)–(2.12) for solving (2.1)–(2.3) consists of following two steps:

Step 1. We first obtain Ψ_j^1 iteratively from a known Ψ_j^0, $j = 1, 2, \ldots, M$. We have

$$-\mathrm{i}\mu\alpha(\Psi_{xx})_j^* + [\lambda_0 - \mathrm{i}\mu P|(\Psi_j^1)_s|^2 - \mathrm{i}\mu V_j](\Psi_j^1)^* = \lambda_0\Psi_j^0 - \mathrm{i}\mu f_j^1, \tag{2.14}$$

$$\begin{aligned}\frac{7}{16}[(\Psi_x)_{j+1}^* + (\Psi_x)_{j-1}^*] + (\Psi_x)_j^* - \frac{h}{16}[(\Psi_{xx})_{j+1}^* - (\Psi_{xx})_{j-1}^*] \\ = \frac{15}{16h}[(\Psi_{j+1}^1)^* - (\Psi_{j-1}^1)^*],\end{aligned} \tag{2.15}$$

$$\begin{aligned}\frac{9}{8h}[(\Psi_x)_{j+1}^* - (\Psi_x)_{j-1}^*] + (\Psi_{xx})_j^* - \frac{1}{8}[(\Psi_{xx})_{j+1}^* + (\Psi_{xx})_{j-1}^*] \\ = \frac{3}{h^2}[(\Psi_{j+1}^1)^* - 2(\Psi_j^1)^* + (\Psi_{j-1}^1)^*],\end{aligned} \tag{2.16}$$

where $(\Psi_j^1)^*$, $(\Psi_x)_j^*$ and $(\Psi_{xx})_j^*$ are the $(s+1)$th iterative solution and derivatives, and $(\Psi_j^1)_s$ is the sth iterative solution for time level one. The initial value for the iteration may be chosen as $(\Psi_j^1)_0 = \Psi_j^0$, and the iteration is carried out until the criterion $\max|(\Psi_j^1)^* - (\Psi_j^1)_s| < 10^{-6}$ is satisfied or the number of the iteration steps is larger than a controlling integer $M \gg 0$, say, $M = 1000$.

Step 2. Once Ψ_j^0 and Ψ_j^1 are available, we proceed for the rest of numerical solutions in the sequence $\{\Psi_j^n\}_{n=2}^N$, $j = 1, 2, \ldots, M$, utilizing the following:

$$\begin{aligned}-\mathrm{i}\mu\alpha(\Psi_{xx})_j^n + [\lambda_0 - \mathrm{i}\mu(P|\Psi_j^e|^2 + V_j)]\Psi_j^n \\ = \sum_{m=1}^{n-1}(\lambda_{n-m-1} - \lambda_{n-m})\Psi_j^m + \lambda_{n-1}\Psi_j^0 - \mathrm{i}\mu f_j^n,\end{aligned} \tag{2.17}$$

$$\begin{aligned}\frac{7}{16}[(\Psi_x)_{j+1}^n + (\Psi_x)_{j-1}^n] + (\Psi_x)_j^n - \frac{h}{16}[(\Psi_{xx})_{j+1}^n - (\Psi_{xx})_{j-1}^n] \\ = \frac{15}{16h}(\Psi_{j+1}^n - \Psi_{j-1}^n),\end{aligned} \tag{2.18}$$

$$\begin{aligned}\frac{9}{8h}[(\Psi_x)_{j+1}^n - (\Psi_x)_{j-1}^n] + (\Psi_{xx})_j^n - \frac{1}{8}[(\Psi_{xx})_{j+1}^n + (\Psi_{xx})_{j-1}^n] \\ = \frac{3}{h^2}(\Psi_{j+1}^n - 2\Psi_j^n + \Psi_{j-1}^n).\end{aligned} \tag{2.19}$$

The coefficient matrices in linear systems in both steps can be rearranged to be triple-tridiagonal, except for several individual elements due to boundary conditions. The

sparse systems can be solved readily via standard triple-forward eliminations and triple-backward substitutions [9].

3. Linear stability analysis

In this section, we focus on the stability of the hybrid $L1$-CCD scheme (2.9)–(2.12). Firstly, we assume that

$$\Psi_j^n = \xi^n(m)\mathrm{e}^{\mathrm{i}\omega j}, \quad (\Psi_{xx})_j^n = \xi_{xx}^n(m)\mathrm{e}^{\mathrm{i}\omega j}, \quad f_j^n = \eta^n(m)\mathrm{e}^{\mathrm{i}\omega j}, \quad \Psi_j^e = \xi^e(m)\mathrm{e}^{\mathrm{i}\omega j}, \tag{3.1}$$

where i, $\xi^n(m)$, $\xi_{xx}^n(m)$ and $\eta^n(m)$ are amplitudes at time level n. Note that $\omega = 2m\pi h/L$ is the phase angle in x-direction [3]. We further observe that

$$\|\Psi^n\|^2 := h\sum_{j=0}^{M}|\Psi_j^n|^2 = \sum_{m=-\infty}^{\infty}|\xi^n(m)|^2,$$
$$\|f^n\|^2 := h\sum_{j=0}^{M}|f_j^n|^2 = \sum_{m=-\infty}^{\infty}|\eta^n(m)|^2$$

due to the Parsevel identity [13]. For the sake of simplicity, we omit m in subsequent discussions. We need the following two lemmas.

Lemma 3.1 ([13], [16])**.** *Let $0 < \gamma < 1$ and λ_l be defined by* (2.6)*. We have*

(1) $1 = \lambda_0 > \lambda_1 > \lambda_2 > \ldots > \lambda_j \to 0$, *as* $j \to \infty$;
(2) $\lambda_{n-1} > (1-\gamma)n^{-\gamma}$.

Lemma 3.2 ([13], [27], [36])**.** *The following is true for amplitudes*

$$\xi_{xx}^n = \frac{\xi^n B}{h^2 A}, \tag{3.2}$$

where $A = 20\cos\omega + 2\cos^2\omega + 23$ *and* $B = 3\ (8\cos\omega + 11\cos^2\omega - 19)$.

Secondly, we may prove:

Theorem 3.1. *The hybrid $L1$-CCD scheme* (2.9)–(2.12) *is unconditionally stable. Moreover, we have*

$$\|\Psi^n\|^2 \leqslant 2\|\Psi^0\|^2 + 2T^{2\gamma}\Gamma^2(1-\gamma)\max_{1\leqslant l\leqslant N}\|f^l\|^2, \quad 1 \leqslant n \leqslant N.$$

P r o o f. For Step 1; that is, $n = 1$, according to (3.1) and Lemma 3.1, if we substitute Ψ_j^1, $(\Psi_{xx})_j^1$ and f_j^1 into (2.14), then

$$(1 - \mathrm{i}\mu P|(\xi^1)_s|^2 - \mathrm{i}\mu V_j)(\xi^1)_{s+1} = \mathrm{i}\mu\alpha(\xi^1_{xx})_{s+1} + \xi^0 - \mathrm{i}\mu\eta^1.$$

Based on Lemma 3.2, we observe that

$$\Big[1 - \mathrm{i}\mu\Big(P|(\xi^1)_s|^2 + V_j + \frac{\alpha B}{h^2 A}\Big)\Big](\xi^1)_{s+1} = \xi^0 - \mathrm{i}\mu\eta^1. \tag{3.3}$$

Note that

$$\Big|1 - \mathrm{i}\mu\Big(\frac{\alpha B}{h^2 A} + P|(\xi^1)_s|^2 + V_j\Big)\Big| \geqslant 1 \quad \text{and} \quad \mu < T^\gamma\Gamma(1-\gamma)\lambda_0 = T^\gamma\Gamma(1-\gamma)$$

due to (2.13) and Lemma 3.1. We arrive at

$$|(\xi^1)_{s+1}| \leqslant |\xi^0| + \mu|\eta^1| < |\xi^0| + T^\gamma\Gamma(1-\gamma)|\eta^1|. \tag{3.4}$$

Square both sides of the above to yield that

$$|(\xi^1)_{s+1}|^2 \leqslant 2|\xi^0|^2 + 2T^{2\gamma}\Gamma^2(1-\gamma)|\eta^1|^2$$

because of the Cauchy-Schwarz inequality. Omit the iteration index $s+1$ for further simplicity in notations. Using induction we obtain immediately that

$$\|\Psi^1\|^2 \leqslant 2\|\Psi^0\|^2 + 2T^{2\gamma}\Gamma^2(1-\gamma)\|f^1\|^2.$$

In Step 2, we substitute Ψ_j^n, Ψ_j^e, $(\Psi_{xx})_j^n$ and f_j^n into (2.17), respectively. These lead to

$$\xi^n - \sum_{m=1}^{n-1}(\lambda_{n-m-1} - \lambda_{n-m})\xi^m - \lambda_{n-1}\xi^0 = \mathrm{i}\mu\alpha\xi^n_{xx} + \mathrm{i}\mu P|\xi^e|^2\xi^n + \mathrm{i}\mu V_j\xi^n - \mathrm{i}\mu\eta^n.$$

Now, recall (3.2) in Lemma 3.2. It is observed that

$$\Big[1 - \mathrm{i}\mu\Big(\frac{\alpha B}{h^2 A} + P|\xi^e|^2 + V_j\Big)\Big]\xi^n = \sum_{m=1}^{n-1}(\lambda_{n-m-1} - \lambda_{n-m})\xi^m + \lambda_{n-1}\xi^0 - \mathrm{i}\mu\eta^n. \tag{3.5}$$

Since

$$\Big|1 - \mathrm{i}\mu\Big(\frac{\alpha B}{h^2 A} + P|\xi^e|^2 + V_j\Big)\Big| \geqslant 1 \quad \text{and} \quad \mu < T^\gamma\Gamma(1-\gamma)\lambda_{n-1},$$

we acquire immediately that

$$|\xi^n| \leqslant \sum_{m=1}^{n-1}(\lambda_{n-m-1}-\lambda_{n-m})|\xi^m| + \lambda_{n-1}[|\xi^0| + T^\gamma\Gamma(1-\gamma)|\eta^n|] \tag{3.6}$$

from (3.5). By the same token, via induction we obtain

$$|\xi^n| \leqslant |\xi^0| + T^\gamma\Gamma(1-\gamma)\max_{1\leqslant k\leqslant N}|\eta^k| \tag{3.7}$$

from (3.6).

Squaring both sides of (3.7), we may find that

$$|\xi^n|^2 \leqslant 2|\xi^0|^2 + 2T^{2\gamma}\Gamma^2(1-\gamma)\max_{1\leqslant k\leqslant N}|\eta^k|^2$$

again due to the Cauchy-Schwarz inequality. Hence,

$$\|\Psi^n\|^2 \leqslant 2\|\Psi^0\|^2 + 2T^{2\gamma}\Gamma^2(1-\gamma)\max_{1\leqslant k\leqslant N}\|f^k\|^2.$$

The above completes our proof. □

Based on Theorem 3.1, we may further prove the following boundedness, or conservative, property in connection with scheme (2.9)–(2.12).

Corollary 3.1. *Let u_j^n, v_j^n and w_j^n be solutions of the following system:*

$$\mathcal{D}_t^\gamma u_j^n = \mathrm{i}\alpha w_j^n + \mathrm{i}P|u_j^e|^2u_j^n + \mathrm{i}V_ju_j^n + f_j^n, \tag{3.8}$$

$$\frac{7}{16}(v_{j+1}^n + v_{j-1}^n) + v_j^n - \frac{h}{16}(w_{j+1}^n - w_{j-1}^n) = \frac{15}{16h}(u_{j+1}^n - u_{j-1}^n) + g_j^n, \tag{3.9}$$

$$\frac{9}{8h}(v_{j+1}^n - v_{j-1}^n) - \frac{1}{8}(w_{j+1}^n + w_{j-1}^n) + w_j^n = \frac{3}{h^2}(u_{j+1}^n - 2u_j^n + u_{j-1}^n) + \tilde{g}_j^n, \tag{3.10}$$

$$u_j^0 = u_0(x_j) \tag{3.11}$$

for $1 \leqslant j \leqslant M$, $1 \leqslant n \leqslant N$. Then

$$\|u^n\|^2 \leqslant 2\|u^0\|^2 + 6T^{2\gamma}\Gamma^2(1-\gamma)\max_{1\leqslant l\leqslant N}\Big(\|f^l\|^2 + \frac{36\alpha^2}{h^2}\|g^l\|^2 + 4\alpha^2\|\tilde{g}^l\|^2\Big).$$

P r o o f. First, we may rewrite the solutions into vector form:

$$u^n=[u_1^n,u_2^n,\dots,u_M^n]^\top,\ v^n=[v_1^n,v_2^n,\dots,v_M^n]^\top,\ w^n=[w_1^n,w_2^n,\dots,w_M^n]^\top,\ 0\leqslant n\leqslant N.$$

Further, we have

$$u^n(x)=\begin{cases}u_j^n, & x_j-\dfrac{h}{2}\leqslant x<x_j+\dfrac{h}{2},\ 1\leqslant j\leqslant M-1,\\[2ex] u_M^n, & x\in\Big[x_M-\dfrac{h}{2},x_M\Big]\cup\Big[x_0,x_0+\dfrac{h}{2}\Big];\end{cases}$$

$$w^n(x)=\begin{cases}w_j^n, & x_j-\dfrac{h}{2}\leqslant x<x_j+\dfrac{h}{2},\ 1\leqslant j\leqslant M-1,\\[2ex] w_M^n, & x\in\Big[x_M-\dfrac{h}{2},x_M\Big]\cup\Big[x_0,x_0+\dfrac{h}{2}\Big];\end{cases}$$

$$v^n(x)=\begin{cases}v_j^n, & x_j-\dfrac{h}{2}\leqslant x<x_j+\dfrac{h}{2},\ 1\leqslant j\leqslant M-1,\\[2ex] v_M^n, & x\in\Big[x_M-\dfrac{h}{2},x_M\Big]\cup\Big[x_0,x_0+\dfrac{h}{2}\Big].\end{cases}$$

Similarly, $u^e(x)$, $f^n(x)$, $g^n(x)$, $\tilde{g}^n(x)$ can be analogously defined.

Next, we expand $u^n(x)$, $u^e(x)$, $v^n(x)$, $w^n(x)$, $f^n(x)$, $g^n(x)$, and $\tilde{g}^n(x)$ into Fourier series on the interval $[0,L]$, that is,

$$u^n(x)=\frac{1}{\sqrt{L}}\sum_{m=-\infty}^{\infty}a_n(m)\mathrm{e}^{\mathrm{i}2\pi mx/L},\quad v^n(x)=\frac{1}{\sqrt{L}}\sum_{m=-\infty}^{\infty}b_n(m)\mathrm{e}^{\mathrm{i}2\pi mx/L},$$

$$w^n(x)=\frac{1}{\sqrt{L}}\sum_{m=-\infty}^{\infty}c_n(m)\mathrm{e}^{\mathrm{i}2\pi mx/L},\quad f^n(x)=\frac{1}{\sqrt{L}}\sum_{m=-\infty}^{\infty}p_n(m)\mathrm{e}^{\mathrm{i}2\pi mx/L},$$

$$g^n(x)=\frac{1}{\sqrt{L}}\sum_{m=-\infty}^{\infty}q_n(m)\mathrm{e}^{\mathrm{i}2\pi mx/L},\quad \tilde{g}^n(x)=\frac{1}{\sqrt{L}}\sum_{m=-\infty}^{\infty}r_n(m)\mathrm{e}^{\mathrm{i}2\pi mx/L},$$

$$u^e(x)=\frac{1}{\sqrt{L}}\sum_{m=-\infty}^{\infty}a_e(m)\mathrm{e}^{\mathrm{i}2\pi mx/L},$$

for $0\leqslant n\leqslant N$, and similarly,

$$a_n(m)=\frac{1}{\sqrt{L}}\int_0^L u^n(x)\mathrm{e}^{-\mathrm{i}2\pi mx/L},\quad b_n(m)=\frac{1}{\sqrt{L}}\int_0^L v^n(x)\mathrm{e}^{-\mathrm{i}2\pi mx/L},$$

$$c_n(m)=\frac{1}{\sqrt{L}}\int_0^L w^n(x)\mathrm{e}^{-\mathrm{i}2\pi mx/L},\quad p_n(m)=\frac{1}{\sqrt{L}}\int_0^L f^n(x)\mathrm{e}^{-\mathrm{i}2\pi mx/L},$$

$$q_n(m)=\frac{1}{\sqrt{L}}\int_0^L g^n(x)\mathrm{e}^{-\mathrm{i}2\pi mx/L},\quad r_n(m)=\frac{1}{\sqrt{L}}\int_0^L \tilde{g}^n(x)\mathrm{e}^{-\mathrm{i}2\pi mx/L},$$

$$a_e(m)=\frac{1}{\sqrt{L}}\int_0^L u^e(x)\mathrm{e}^{-\mathrm{i}2\pi mx/L},$$

for $0 \leqslant n \leqslant N$. Thus, by the definition of the L^2-norm and the Parseval equality, we have

$$\|u^n(x)\|^2 = \int_0^L |u^n(x)|^2 \,\mathrm{d}x = \sum_{m=-\infty}^{\infty} |a_n(m)|^2.$$

Subsequently,

$$\begin{aligned}\|u^n\|^2 = h\sum_{j=1}^{M}(u_j^n)^2 = \int_{x_0}^{x_0+h/2} [u^n(x)]^2 \,\mathrm{d}x + \sum_{j=1}^{M-1}\int_{x_j-h/2}^{x_j+h/2} [u^n(x)]^2 \,\mathrm{d}x \\ + \int_{x_M-h/2}^{x_M} [u^n(x)]^2 \,\mathrm{d}x = \|u^n(x)\|^2.\end{aligned}$$

From the above discussions we may derive that

$$\|u^n\|^2 = \sum_{m=-\infty}^{\infty} |a_n(m)|^2.$$

By the same token, we may find that

$$\begin{aligned}&\|v^n\|^2 = \sum_{m=-\infty}^{\infty} |b_n(m)|^2, \quad \|w^n\|^2 = \sum_{m=-\infty}^{\infty} |c_n(m)|^2, \quad \|f^n\|^2 = \sum_{m=-\infty}^{\infty} |p_n(m)|^2,\\ &\|g^n\|^2 = \sum_{m=-\infty}^{\infty} |q_n(m)|^2, \quad \|\tilde{g}^n\|^2 = \sum_{m=-\infty}^{\infty} |r_n(m)|^2, \quad \|u^e\|^2 = \sum_{m=-\infty}^{\infty} |a_e(m)|^2.\end{aligned}$$

Thus, we have

$$\begin{aligned}&u_j^n = \frac{1}{\sqrt{L}} a_n \mathrm{e}^{\mathrm{i}\varrho jh}, \quad w_j^n = \frac{1}{\sqrt{L}} c_n \mathrm{e}^{\mathrm{i}\varrho jh}, \quad v_j^n = \frac{1}{\sqrt{L}} b_n \mathrm{e}^{\mathrm{i}\varrho jh},\\ &f_j^n = \frac{1}{\sqrt{L}} p_n \mathrm{e}^{\mathrm{i}\varrho jh}, \quad g_j^n = \frac{1}{\sqrt{L}} q_n \mathrm{e}^{\mathrm{i}\varrho jh}, \quad \tilde{g}_j^n = \frac{1}{\sqrt{L}} r_n \mathrm{e}^{\mathrm{i}\varrho jh}, \quad u_j^e = \frac{1}{\sqrt{L}} a_e \mathrm{e}^{\mathrm{i}\varrho jh},\end{aligned}$$

where $\varrho = 2m\pi/L$.

Now, recall (3.9), (3.10). For $1 \leqslant n \leqslant N$ we must have

$$\begin{aligned}\Big[1 + \frac{7}{8}\cos(\varrho h)\Big] b_n - \mathrm{i}\frac{h}{8}\sin(\varrho h) c_n = \mathrm{i}\frac{15}{8h}\sin(\varrho h) a_n + q_n,\\ \mathrm{i}\frac{9}{4h}\sin(\varrho h) b_n + \Big[1 - \frac{1}{4}\cos(\varrho h)\Big] c_n = \frac{6}{h^2}[\cos(\varrho h) - 1] a_n + r_n.\end{aligned}$$

After some straightforward calculations, we obtain

$$b_n = \mathrm{i}\frac{1}{h}\beta_1(\cos(\varrho h), \sin(\varrho h)) a_n + \mathrm{i}\varrho_1(\cos(\varrho h), \sin(\varrho h)) r_n + \sigma_1 \cos(\varrho h) q_n, \tag{3.12}$$

$$c_n = \frac{1}{h^2}\beta_2 \cos(\varrho h) a_n + \varrho_2 \cos(\varrho h) r_n - \mathrm{i}\sigma_2(\cos(\varrho h), \sin(\varrho h)) q_n, \tag{3.13}$$

in which

$$\beta_1(x,y)=\frac{36y+9xy}{2x^2+20x+23},\quad \varrho_1(x,y)=\frac{4hy}{2x^2+20x+23},\quad \sigma_1(x)=\frac{-8x+32}{2x^2+20x+23},$$
$$\beta_2(x)=\frac{33x^2+24x-57}{2x^2+20x+23},\quad \varrho_2(x)=\frac{28x+32}{2x^2+20x+23},\ \sigma_2(x,y)=\frac{72y/h}{2x^2+20x+23}.$$

It is readily observable that, when $x\in[-1,1]$,

$$\beta_2'(x)=\frac{612x^2+1746x+1692}{(2x^2+20x+23)^2}>0.$$

Hence $\beta_2(x)$ is monotonically increasing in $[-1,1]$, and subsequently,

$$-\frac{48}{5}\leqslant\beta_2\cos(\varrho h)\leqslant 0.$$

In addition, we may observe that

$$\frac{4}{5}\leqslant\varrho_2\cos(\varrho h)\leqslant 2-\frac{1}{3}\sqrt{\frac{10}{3}}<2, \tag{3.14}$$

$$|\sigma_2(\cos(\varrho h),\sin(\varrho h))|\leqslant\frac{6}{h}. \tag{3.15}$$

Thus, according to (3.8), the following must be true:

$$\frac{1}{\Gamma(2-\gamma)\tau^\gamma}\bigg[a_n-\sum_{l=1}^{n-1}(\lambda_{n-l-1}-\lambda_{n-l})a_l-\lambda_{n-1}a_0\bigg] \tag{3.16}$$
$$=\mathrm{i}\alpha c_n+\mathrm{i}P|a_e|^2a_n+\mathrm{i}V_ja_n+p_n,\quad 1\leqslant n\leqslant N.$$

A substitution of (3.13) into (3.16) leads to

$$\bigg[1-\frac{\mathrm{i}\alpha\mu}{h^2}\beta_2\cos(\varrho h)-\mathrm{i}\mu P|a_e|^2-\mathrm{i}\mu V_j\bigg]a_n=\sum_{l=1}^{n-1}(\lambda_{n-l-1}-\lambda_{n-l})a_l+\lambda_{n-1}a_0$$
$$+\mu p_n+\mathrm{i}\alpha\mu\varrho_2(\cos(\varrho h))r_n+\alpha\mu\sigma_2(\cos(\varrho h),\sin(\varrho h))q_n,\ 1\leqslant n\leqslant N,$$

due to the fact that $\mu=\tau^\gamma\Gamma(2-\gamma)$. On the other hand, we observe that

$$\bigg|1-\frac{\mathrm{i}\alpha\mu}{h^2}\beta_2\cos(\varrho h)-\mathrm{i}\mu P|a_e|^2-\mathrm{i}\mu V_j\bigg|\geqslant 1.$$

Therefore, the following must be true:

$$|a_n|\leqslant\sum_{l=1}^{n-1}(\lambda_{n-l-1}-\lambda_{n-l})|a_l|+\lambda_{n-1}|a_0|$$
$$+\mu[|p_n|+|\alpha\varrho_2\cos(\varrho h)||r_n|+|\alpha\sigma_2(\cos(\varrho h),\sin(\varrho h))||q_n|],\quad 1\leqslant n\leqslant N.$$

Now, according to Lemma 3.1, we have

$$\mu = \tau^{\gamma}\Gamma(2-\gamma) = (n\tau)^{\gamma}\Gamma(1-\gamma)k^{-\gamma}(1-\gamma) < T^{\gamma}\Gamma(1-\gamma)\lambda_{n-1}.$$

Therefore,

$$|a_n| \leqslant \sum_{l=1}^{n-1}(\lambda_{n-l-1}-\lambda_{n-l})|a_l| + \lambda_{n-1}\Theta_n, \quad 1 \leqslant n \leqslant N, \tag{3.17}$$

where

$$\Theta_n = |a_0| + T^{\gamma}\Gamma(1-\gamma)[|p_n| + |\alpha\varrho_2(\cos(\varrho h))||r_n| + |\alpha\sigma_2(\cos(\varrho h),\sin(\varrho h))||q_n|].$$

Square both sides of (3.17). By the Cauchy-Schwartz inequality, we conclude immediately that

$$|a_n|^2 \leqslant \sum_{l=1}^{n-1}(\lambda_{n-l-1}-\lambda_{n-l})|a_l|^2 + \lambda_{n-1}\Theta_n^2, \quad 1 \leqslant n \leqslant N, \tag{3.18}$$

together with

$$\Theta_n^2 \leqslant 2|a_0|^2 + 6T^{2\gamma}\Gamma^2(1-\gamma)[|p_n|^2 + \alpha^2\varrho_2^2\cos(\varrho h)|r_n|^2 + \alpha^2\sigma_2^2(\cos(\varrho h),\sin(\varrho h))|q_n|^2].$$

Because of (3.18), we acquire that

$$\|u^n\|^2 \leqslant \sum_{l=1}^{n-1}(\lambda_{n-l-1}-\lambda_{n-l})\|u^l\|^2 + \lambda_{n-1}\Phi, \quad 1 \leqslant n \leqslant N,$$

where

$$\Phi = 2\|u^0\|^2 + 6T^{2\gamma}\Gamma^2(1-\gamma)\Big[\max_{1\leqslant l\leqslant N}\|f^l\|^2 + \alpha^2\varrho_2^2\cos(\varrho h)\|\tilde{g}^l\|^2 + \alpha^2\sigma_2^2(\cos(\varrho h),\sin(\varrho h))\|g^l\|^2\Big].$$

Utilizing an induction again, we find that

$$\|u^n\|^2 \leqslant \Phi, \quad 1 \leqslant n \leqslant N.$$

Finally, by applying (3.14) and (3.15), the following inequalities must hold,

$$\varrho_2^2\cos(\varrho h) \leqslant 4,$$
$$\sigma_2^2(\cos(\varrho h),\sin(\varrho h)) \leqslant \frac{36}{h^2}.$$

The above evidently completes our proof. □

4. Numerical experiments

We consider two typical computational examples in this section. All experiments are carried out utilizing `Matlab` 7.10 on `Dell` Vostro 260s workstations with 3.1GHz `Intel` Core i5-2400 CPU and 4GB RAM installed.

Numerical errors are evaluated under the ℓ_∞ norm, that is,

$$\mathrm{Error}(h,\tau) = \|\Psi - \Psi_{\mathrm{exact}}\|_\infty.$$

Relative rates of convergences [22], [42] are calculated in the sense that

$$\mathrm{Rate}_h = \log_2 \frac{\mathrm{Error}(h,\tau)}{\mathrm{Error}(\frac{1}{2}h,\tau)}, \quad \mathrm{Rate}_\tau = \log_2 \frac{\mathrm{Error}(h,\tau)}{\mathrm{Error}(h,\frac{1}{2}\tau)}.$$

Example 4.1. Consider the following initial-boundary value problem with a cubic nonlinearity (see [3], [40])

$$\begin{gathered}
\mathrm{i}\frac{\partial^\gamma \Psi}{\partial t^\gamma} + \frac{\partial^2 \Psi}{\partial x^2} + |\Psi|^2\Psi = f(x,t), \quad 0 < x < 1,\ 0 < t \leqslant 1,\\
\Psi(x,0) = 0, \quad 0 \leqslant x \leqslant 1,\\
\Psi(0,t) = \Psi(1,t) = \mathrm{i}t^2, \quad 0 < t \leqslant 1,
\end{gathered}$$

where

$$f(x,t) = \Big(-\frac{2t^{2-\gamma}}{\Gamma(3-\gamma)} + (-4\pi^2 t^2 + t^6)\mathrm{i}\Big)\mathrm{e}^{-2\pi x\mathrm{i}}, \quad 0 < x < 1,\ 0 < t \leqslant 1.$$

The exact solution of the above problem is

$$\Psi(x,t) = \mathrm{i}t^2\mathrm{e}^{-2\pi x\mathrm{i}}, \quad 0 \leqslant x \leqslant 1,\ 0 \leqslant t \leqslant 1.$$

Table 1 is devoted to the spatial accuracy of the underlying numerical method. An order six accuracy in space can be rendered from the numerical results exhibited. Table 2 is on the other hand for the temporal accuracy of our hybrid $L1$-CCD method (2.9)–(2.12). Again, the anticipated accuracy is confirmed for various values of γ used.

M	$\gamma = 0.1$		$\gamma = 0.3$		$\gamma = 0.5$	
	$\mathrm{Error}(h,\tau)$	Rate_h	$\mathrm{Error}(h,\tau)$	Rate_h	$\mathrm{Error}(h,\tau)$	Rate_h
4	4.7367×10^{-3}	—	4.7359×10^{-3}	—	4.7349×10^{-3}	—
8	6.6680×10^{-5}	6.1505	6.6668×10^{-5}	6.1505	6.6655×10^{-5}	6.1505
16	1.0084×10^{-6}	6.0472	1.0082×10^{-6}	6.0472	1.0080×10^{-6}	6.0472
32	1.5631×10^{-8}	6.0115	1.5628×10^{-8}	6.0115	1.5635×10^{-8}	6.0106

Table 1. Errors and estimated spatial convergence rates for Example 4.1. Fractional orders $\gamma = 0.1$, 0.3, 0.5 and the temporal step $\tau = 1/120\,000$ are used, respectively.

τ	$\gamma = 0.1$		$\gamma = 0.6$		$\gamma = 0.75$	
	$\mathrm{Error}(h,\tau)$	Rate_τ	$\mathrm{Error}(h,\tau)$	Rate_τ	$\mathrm{Error}(h,\tau)$	Rate_τ
1/50	4.3840×10^{-5}	—	7.5797×10^{-5}	—	1.4733×10^{-4}	—
1/100	1.0969×10^{-5}	1.9988	2.5734×10^{-5}	1.5585	5.9753×10^{-5}	1.3020
1/200	2.7435×10^{-6}	1.9994	9.1992×10^{-6}	1.4841	2.4744×10^{-5}	1.2719
1/400	6.8614×10^{-7}	1.9994	3.3869×10^{-6}	1.4416	1.0336×10^{-5}	1.2595

Table 2. Errors and estimated temporal rates of convergence for Example 4.1. Fractional orders $\gamma = 0.1$, 0.6, 0.75 and $h = \pi/100$ are used, respectively.

Further, Figure 1 shows the numerical as well as the exact solutions. Real and imaginary parts corresponding to $\gamma = 0.3$, $M = 32$ are plotted with $\tau = 1/120\,000$. The figures indicate not only acceptable agreement between the solutions, but also effectiveness of the proposed novel compact algorithm.

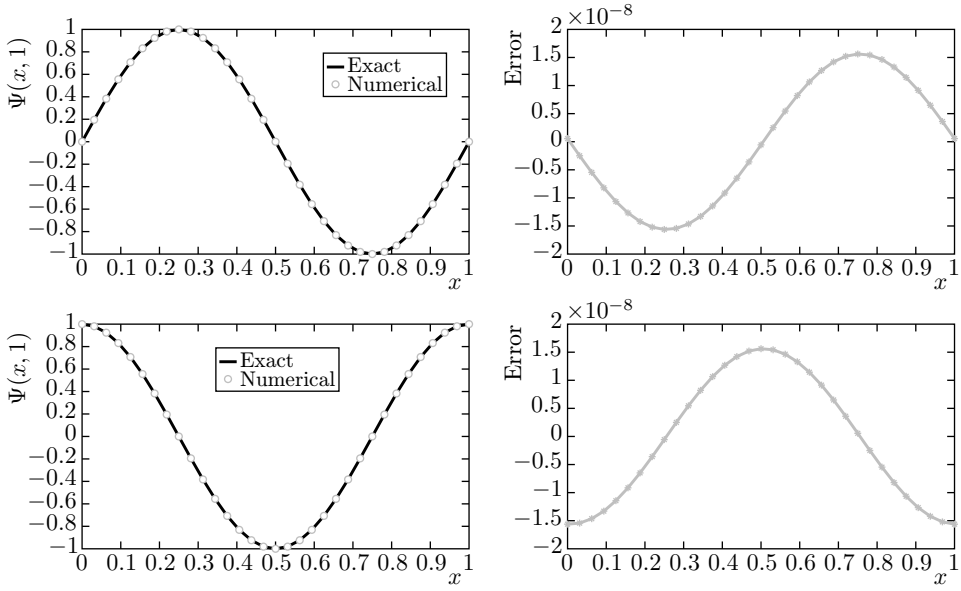

Figure 1. Numerical and exact solutions together with errors for the real part (first row) and imaginary part (second row) for Example 4.1.

E x a m p l e 4.2. To explore further the superiorities of our hybrid high order method, let us now consider a typical testing NTFSE with a trapping potential (see [2])

$$\mathrm{i}\frac{\partial^\gamma \Psi}{\partial t^\gamma} + \frac{\partial^2 \Psi}{\partial x^2} + |\Psi|^2\Psi + \cos^2 x\Psi = f(x,t), \quad 0 < x < \pi,\ 0 < t \leqslant 1,$$
$$\Psi(x,0) = 0, \quad 0 \leqslant x \leqslant \pi,$$
$$\Psi(0,t) = \Psi(\pi,t) = t^3, \quad 0 < t \leqslant 1,$$

where

$$f(x,t) = \Big(\mathrm{i}\frac{6t^{3-\gamma}}{\Gamma(4-\gamma)} - 4t^3 + t^9 + t^3\cos^2 x\Big)\mathrm{e}^{2x\mathrm{i}}, \quad 0 < x < \pi,\ 0 < t \leqslant 1.$$

The exact solution in this case is

$$\Psi(x,t) = t^3\mathrm{e}^{2x\mathrm{i}}, \quad 0 \leqslant x \leqslant \pi,\ 0 \leqslant t \leqslant 1.$$

In Table 3, the real and imaginary parts of the numerical solutions are again considered separately [2]. A sixth-order spatial accuracy can be observed. Again, the estimates are satisfactory. We further present the estimated temporal accuracy in Table 4. Figure 2 is devoted to the exact solution and its numerical approximation acquired by our $L1$-CCD scheme with separated real and imaginary parts. Parameters $\gamma = 0.5$, $M = 32$ and $\tau = 1/120\,000$ are utilized. It is evident again that the desired accuracies are achieved by our new computational method.

γ	M	Real part		Imaginary part	
		Error(h,τ)	Rate$_h$	Error(h,τ)	Rate$_h$
$\gamma = 0.1$	4	1.5275×10^{-2}	—	1.4561×10^{-2}	—
	8	2.3992×10^{-4}	5.9924	2.2429×10^{-4}	6.0206
	16	3.7621×10^{-6}	5.9949	3.5375×10^{-6}	5.9865
	32	5.9062×10^{-8}	5.9932	5.5532×10^{-8}	5.9933
$\gamma = 0.3$	4	0.9524×10^{-2}	—	0.8912×10^{-2}	—
	8	1.6316×10^{-4}	5.8671	1.5332×10^{-4}	5.8610
	16	2.4680×10^{-6}	6.0478	2.3192×10^{-6}	6.0468
	32	3.8722×10^{-8}	5.9940	3.6321×10^{-8}	5.9967
$\gamma = 0.5$	4	0.6273×10^{-2}	—	0.5794×10^{-2}	—
	8	1.1696×10^{-4}	5.7449	1.1137×10^{-4}	5.7012
	16	1.7688×10^{-6}	6.0484	1.6828×10^{-6}	6.0484
	32	2.9218×10^{-8}	5.9197	2.7889×10^{-8}	5.9150

Table 3. Errors and rates of spatial convergence for Example 4.2. Parameters $\gamma = 0.1$, 0.3, 0.5 and $\tau = 1/120\,000$ are used.

M	$\gamma = 0.1$		$\gamma = 0.6$		$\gamma = 0.75$	
	Error(h,τ)	Rate$_h$	Error(h,τ)	Rate$_h$	Error(h,τ)	Rate$_h$
1/50	4.1000×10^{-3}	—	2.8383×10^{-3}	—	5.5870×10^{-3}	—
1/100	1.1000×10^{-3}	1.8733	9.8161×10^{-4}	1.5318	2.2794×10^{-3}	1.2934
1/200	2.8684×10^{-4}	1.9468	3.5326×10^{-4}	1.4744	9.4263×10^{-4}	1.2739
1/400	7.2593×10^{-5}	1.9824	1.3017×10^{-4}	1.4404	3.9264×10^{-4}	1.2635

Table 4. Errors and temporal rates of convergence for Example 4.2. Parameters $\gamma = 0.1$, 0.6, 0.75 and $h = \pi/100$ are incorporated.

5. Conclusion

A high-order $L1$-CCD hybrid numerical method for solving time fractional order NTFSEs is developed, analyzed and discussed. Proper linearization procedures are used to effectively improve the overall efficiency. The novel new computational strategy provides an accuracy of order six in space and order $2-\gamma$ in time, respectively, where $0 < \gamma < 1$ is the fractional derivative order. It is proved rigorously that the numerical scheme is unconditionally stable in the Fourier sense. An interesting boundedness result is discussed. Two typical testing examples are given and computational experiments are carried out to illustrate the accuracy and effectiveness of the proposed hybrid method. Order six convergence is continuously observed in simulation experiments.

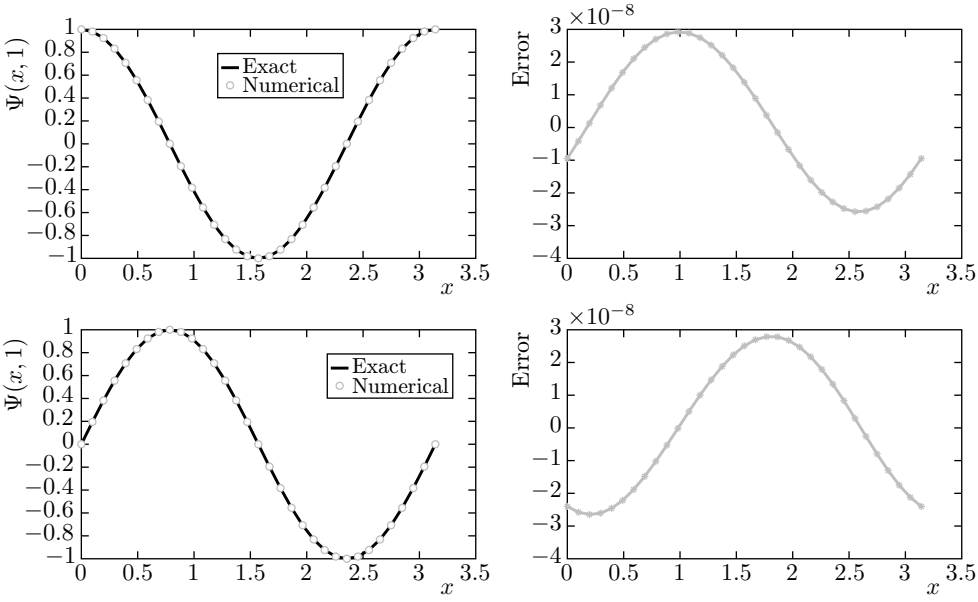

Figure 2. Numerical and exact solutions, their errors in real part (first row) and imaginary part (second row) for Example 4.2.

Our continuing work is to extend the current hybrid $L1$-CCD method for solving more general and sophisticated nonlinear fractional partial differential equations, in particular the Helmholtz equations at high wave numbers [22]. We have just accomplished successful initial approaches based on CCD and even-higher order $L1$-2 combined schemes for theoretical analysis [17]. Careful numerical analysis of the convergence of hybrid class of CCD schemes have been in progress. Superconvergence and blow-up adaptive methods have also been approached [15], [25], [42].

A c k n o w l e d g m e n t s . The authors would like to thank the anonymous referees for their time spent and extremely valuable remarks given. Their suggestions have significantly improved the quality and presentation of this paper. The last author appreciates particularly the M3HPCST-2020 conference and its organizers. Last but not least, the authors would also thank the editor for the tremendous amount of encouragement received throughout the preparation of this article.

References

[1] *D. Baleanu, K. Diethelm, E. Scalas, J. J. Trujillo*: Fractional Calculus: Models and Numerical Methods. Series on Complexity, Nonlinearity and Chaos 5. World Scientific, Hackensack, 2012. zbl MR doi

[2] *D. A. Benson, R. Schumer, M. M. Meerschaert, S. W. Wheatcraft*: Fractional dispersion, Lévy motion, and the MADE tracer tests. Transp. Porous Media *42* (2001), 211–240. MR doi

[3] *A. H. Bhrawy, E. H. Doha, S. S. Ezz-Eldien, R. A. Van Gorder*: A new Jacobi spectral collocation method for solving 1+1 fractional Schrödinger equations and fractional coupled Schrödinger systems. Eur. Phys. J. Plus *129* (2014), Article ID 260, 21 pages. doi

[4] *A. G. Bratsos*: A linearized finite-difference scheme for the numerical solution of the nonlinear cubic Schrödinger equation. Korean J. Comput. Appl. Math. *8* (2001), 459–467. zbl MR doi

[5] *Q. Chang, E. Jia, W. Sun*: Difference schemes for solving the generalized nonlinear Schrödinger equation. J. Comput. Phys. *148* (1999), 397–415. zbl MR doi

[6] *X. Chen, Y. Di, J. Duan, D. Li*: Linearized compact ADI schemes for nonlinear time-fractional Schrödinger equations. Appl. Math. Lett. *84* (2018), 160–167. zbl MR doi

[7] *B. Chen, D. He, K. Pan*: A linearized high-order combined compact difference scheme for multi-dimensional coupled Burgers' equations. Numer. Math., Theory Methods Appl. *11* (2018), 299–320. zbl MR doi

[8] *B. Chen, D. He, K. Pan*: A CCD-ADI method for two-dimensional linear and nonlinear hyperbolic telegraph equations with variable coefficients. Int. J. Comput. Math. *96* (2019), 992–1004. MR doi

[9] *P. C. Chu, C. Fan*: A three-point combined compact difference scheme. J. Comput. Phys. *140* (1998), 370–399. zbl MR doi

[10] *M. Cui*: Compact finite difference method for the fractional diffusion equation. J. Comput. Phys. *228* (2009), 7792–7804. zbl MR doi

[11] *M. Dehghan, A. Taleei*: A compact split-step finite difference method for solving the nonlinear Schrödinger equations with constant and variable coefficients. Comput. Phys. Commun. *181* (2010), 43–51. zbl MR doi

[12] *R. P. Feynman, A. R. Hibbs*: Quantum Mechanics and Path Integrals. Dover Publications, New York, 2010. zbl MR

[13] *G.-H. Gao, H.-W. Sun*: Three-point combined compact alternating direction implicit difference schemes for two-dimensional time-fractional advection-diffusion equations. Commun. Comput. Phys. *17* (2015), 487–509. zbl MR doi

[14] *G.-H. Gao, H.-W. Sun*: Three-point combined compact difference schemes for time-fractional advection-diffusion equations with smooth solutions. J. Comput. Phys. *298* (2015), 520–538. zbl MR doi

[15] *G.-H. Gao, H.-W. Sun, Z.-Z. Sun*: Stability and convergence of finite difference schemes for a class of time-fractional sub-diffusion equations based on certain superconvergence. J. Comput. Phys. *280* (2015), 510–528. zbl MR doi

[16] *G.-H. Gao, Z.-Z. Sun*: A compact finite difference scheme for the fractional sub-diffusion equations. J. Comput. Phys. *230* (2011), 586–595. zbl MR doi
[17] *G.-H. Gao, Z.-Z. Sun, H.-W. Zhang*: A new fractional numerical differentiation formula to approximate the Caputo fractional derivative and its applications. J. Comput. Phys. *259* (2014), 33–50. zbl MR doi
[18] *A. K. Golmankhaneh, D. Baleanu*: Calculus on fractals. Fractional Dynamics. De Gruyter, Berlin, 2015, pp. 307–332. zbl MR doi
[19] *D. He*: An unconditionally stable spatial sixth-order CCD-ADI method for the two-dimensional linear telegraph equation. Numer. Algorithms *72* (2016), 1103–1117. zbl MR doi
[20] *D. He, K. Pan*: A fifth-order combined compact difference scheme for the Stokes flow on polar geometries. East Asian J. Appl. Math. *7* (2017), 714–727. zbl MR doi
[21] *D. He, K. Pan*: An unconditionally stable linearized CCD-ADI method for generalized nonlinear Schrödinger equations with variable coefficients in two and three dimensions. Comput. Math. Appl. *73* (2017), 2360–2374. zbl MR doi
[22] *T. N. Jones, Q. Sheng*: Asymptotic stability of a dual-scale compact method for approximating highly oscillatory Helmholtz solutions. J. Comput. Phys. *392* (2019), 403–418. MR doi
[23] *N. A. Khan, M. Jamil, A. Ara*: Approximate solutions to time-fractional Schrödinger equation via homotopy analysis method. Int. Sch. Res. Not. *2012* (2012), Article ID 197068, 11 pages. doi
[24] *R. Klages, G. Radons, I. M. Sokolov* (eds.): Anomalous Transport: Foundations and Applications. Wiley, Weinheim, 2008. doi
[25] *N. Laskin*: Fractional quantum mechanics and Lévy path integrals. Phys. Lett., A *268* (2000), 298–305. zbl MR doi
[26] *S. T. Lee, J. Liu, H.-W. Sun*: Combined compact difference scheme for linear second-order partial differential equations with mixed derivative. J. Comput. Appl. Math. *264* (2014), 23–37. zbl MR doi
[27] *L. Z. Li, H.-W. Sun, S.-C. Tam*: A spatial sixth-order alternating direction implicit method for two-dimensional cubic nonlinear Schrödinger equations. Comput. Phys. Commun. *187* (2015), 38–48. zbl MR doi
[28] *D. Li, J. Wang, J. Zhang*: Unconditionally convergent $L1$-Galerkin FEMs for nonlinear time-fractional Schrödinger equations. SIAM. J. Sci. Comput. *39* (2017), A3067–A3088. zbl MR doi
[29] *H.-L. Liao, H.-S. Shi, Y. Zhao*: Numerical study of fourth-order linearized compact schemes for generalized NLS equations. Comput. Phys. Commun. *185* (2014), 2240–2249. zbl MR doi
[30] *A. Mohebbi, M. Abbaszadeh, M. Dehghan*: The use of a meshless technique based on collocation and radial basis functions for solving the time fractional nonlinear Schrödinger equation arising in quantum mechanics. Eng. Anal. Bound. Elem. *37* (2013), 475–485. zbl MR doi
[31] *D. A. Murio*: Implicit finite difference approximation for time fractional diffusion equations. Comput. Math. Appl. *56* (2008), 1138–1145. zbl MR doi
[32] *M. Naber*: Time fractional Schrödinger equation. J. Math. Phys. *45* (2004), 3339–3352. zbl MR doi
[33] *S. Z. Rida, H. M. El-Sherbiny, A. A. M. Arafa*: On the solution of the fractional nonlinear Schrödinger equation. Phys. Lett., A *372* (2008), 553–558. zbl MR doi
[34] *E. Scalas, R. Gorenflo, F. Mainardi*: Fractional calculus and continuous-time finance. Phys. A *284* (2000), 376–384. MR doi
[35] *E. Shivanian, A. Jafarabadi*: Error and stability analysis of numerical solution for the time fractional nonlinear Schrödinger equation on scattered data of general-shaped domains. Numer. Methods Partial Differ. Equations *33* (2017), 1043–1069. zbl MR doi
[36] *H.-W. Sun, L. Z. Li*: A CCD-ADI method for unsteady convection-diffusion equations. Comput. Phys. Commun. *185* (2014), 790–797. zbl MR doi

[37] *Z.-Z. Sun, X. Wu*: A fully discrete difference scheme for a diffusion-wave system. Appl. Numer. Math. *56* (2006), 193–209. zbl MR doi
[38] *Y.-M. Wang, L. Ren*: Efficient compact finite difference methods for a class of time-fractional convection-reaction-diffusion equations with variable coefficients. Int. J. Comput. Math. *96* (2019), 264–297. MR doi
[39] *Z. Wang, S. Vong*: Compact difference schemes for the modified anomalous fractional sub-diffusion equation and the fractional diffusion-wave equation. J. Comput. Phys. *277* (2014), 1–15. zbl MR doi
[40] *L. Wei, Y. He, X. Zhang, S. Wang*: Analysis of an implicit fully discrete local discontinuous Galerkin method for the time-fractional Schrödinger equation. Finite Elem. Anal. Des. *59* (2012), 28–34. MR doi
[41] *Y. Xu, L. Zhang*: Alternating direction implicit method for solving two-dimensional cubic nonlinear Schrödinger equation. Comput. Phys. Commun. *183* (2012), 1082–1093. zbl MR doi
[42] *L. Zhu, Q. Sheng*: A note on the adaptive numerical solution of a Riemann-Liouville space-fractional Kawarada problem. J. Comput. Appl. Math. *374* (2020), Article ID 112714, 14 pages. zbl MR doi

Authors' addresses: *Chun-Hua Zhang,* Department of Mathematics, University of Macau, Avenida da Universidade, Taipa, Macau, China, e-mail: chzringlang@163.com; *Jun-Wei Jin*, Key Laboratory of Grain Information Processing and Control, Ministry of Education of China, and College of Information Science and Engineering, Henan University of Technology, Zhengzhou 450001, China, e-mail: jinjunwei24@163.com; *Hai-Wei Sun*, Department of Mathematics, University of Macau, Avenida da Universidade, Taipa, Macau, China, e-mail: hsun@um.edu.mo; *Qin Sheng* (corresponding author), Department of Mathematics and Center for Astrophysics, Space Physics and Engineering Research, Baylor University, Waco, TX 76798-7328, USA, e-mail: Qin_Sheng@baylor.edu.